Thermal Destruction of Carbon Black Network Structure in Natural Rubber Vulcanizate

Atsushi Kato,[1] Toshiya Suda,[1] Yuko Ikeda,[2] Shinzo Kohjiya[3]

[1]*NISSAN ARC, LTD., 1 Natsushima-cho, Yokosuka, Kanagawa 237-0061, Japan*
[2]*Kyoto Institute of Technology, Department of Chemistry and Materials Technology, Graduate School of Science and Technology, Hashigami-cho, Matsugasaki, Sakyo-ku, Kyoto 606-8585, Japan*
[3]*Mahidol University, Department of Chemistry, Faculty of Science, Salaya Campus, Phuthamonthon, Nakhonpathom 73170, Thailand*

Received 21 February 2010; accepted 23 November 2010
DOI 10.1002/app.33888
Published online 23 May 2011 in Wiley Online Library (wileyonlinelibrary.com).

ABSTRACT: To investigate thermal destruction and rearrangement of the carbon black (CB) network consisting of CB aggregates in rubbery matrix, the proper heat-treatment temperature without thermal decomposition of rubber matrix were examined by using differential scanning calorimetry, dynamic mechanical measurements, and thermal expansion measurements. 383 K was chosen as the heat-treatment temperature under vacuum. The volume resistivity (ρ_v) of 50 phr CB-filled natural rubber vulcanizate (CB-50) increased rapidly up to a heat-treatment time of 24 h and it decreased by further heat-treatment time, whereas the ρ_v of CB-80 remained almost constant without depending on heating time. Three-dimensional electron microscope (3D-TEM) observations revealed that after the heat-treatment for 75 h, the average lengths of the crosslinked and the branched chains and the crosslinked points density (D_{cross}) of the CB network decreased, whereas the branched points density (D_{branch}) increased with decrease of D_{cross}. After the heat-treatment, their fractions (F_{cross}'s) of crosslinked chains decreased, whereas their fractions (F_{branch}'s) of the branched ones increased. Especially, F_{branch} of CB-50 became larger than that of CB-80, while the decrease of F_{cross} of CB-50 was almost the same as that of CB-80 by the heat-treatment. And, F_{cross} and F_{branch} of the heat-treated CB-50 were the same compositions (F_{cross} and F_{branch} = ca. 0.7 and ca. 0.3, respectively) as those of the heat-treated CB-80. It is suggested that the CB network of CB-80 is more thermal stable than that of CB-50. These results directly indicate that CB network is broken and is rearranged by a heat-treatment. © 2011 Wiley Periodicals, Inc. J Appl Polym Sci 122: 1300–1315, 2011

Key words: natural rubber vulcanizate; carbon black; aggregate; carbon black network; 3D-TEM; heat-treatment

INTRODUCTION

In the field of polymer composite materials, the structure of the dispersed filler in the polymer matrix has not been elucidated enough to even quantitatively predict the mechanical properties of the composites from the structure. This means that the relationship between filler dispersion in the polymer matrix and mechanical properties of polymer composites has not been established yet. For instance, even the well-known reinforcement effect obtained by mixing carbon black (CB) with rubber has not been fully explained.[1,2] Though it is well known that the reinforcement effect may be related to the amount of filler gel in the rubber before vulcanization,[3–5] the structure and morphology of the filler gel in rubber vulcanizates are still not clearly understood. We know that there is a bound rubber layer of several nm in thickness near the surface of CB and that this bound rubber is closely related to the filler gel.[3–5] Even though the bound rubber has been studied much by using the nuclear magnetic resonance (NMR) relaxation time (T_2)[6–9] and tangent loss (tan δ) of dynamic viscoelasticity,[10] no one has been able to confirm exactly where the bound rubber is in CB-filled rubber vulcanizates and to examine its effect on mechanical properties.

We now know that rubber vulcanizates filled with a filler (CB or particulate silica) have a double network structure, i.e., a rubber chain network and a filler network.[11–13] The former can be estimated by the equilibrium degree of swelling by a solvent and the equilibrium modulus of the rubber vulcanizate.[14–16] In the case of the latter, the present authors have succeeded in observing the filler (CB and silica) network structure by means of three-dimensional electron microscopy/tomography (3D-TEM).[17–21] The skeleton of the filler network has been visualized for the first time by combining the closest distance (d_p) between the centers of gravity of two neighboring filler aggregates which is calculated from a 3D-TEM image and the electric percolation behavior of the filler-filled rubber vulcanizate.[17–19]

Correspondence to: A. Kato (kato@nissan-arc.co.jp).

© 2011 Wiley Periodicals, Inc.

On the basis of the visualization results, it was found that local filler aggregates were connected with/to one another to result in a dramatic decrease of the volume resistivity in a relatively low filler loading region. When the volume resistivity reaches almost a constant value in a high CB loading region, a three-dimensional filler network is formed. The filler network is the three-dimensional structure in which the filler aggregates are interconnected with the bound rubber layer around the aggregate. The filler network is consisting of crosslinked and branched chains of the aggregates, and isolated chains are also observed. Surprisingly, it is especially notable that a linear relationship was observed between the fraction of the CB network chain and the fraction of the dielectric relaxation strength of the filler-filled rubber vulcanizate.[19]

It has been known that the filler network is ruptured and rearranged by an external stimulation such as large deformation, heat treatment and so on. Satoh et al. reported that the change in the dynamic modulus for unfilled SBR was reversible under a large compression followed by recovery, while that for the CB-filled samples was irreversible. These results are suggesting a change in filler network at large deformation.[22] It is known that filler network is considered to be much weaker than chemical network.[23–25] Therefore, they thought that filler network may be ruptured in part at large elongation, whereas the junction point in chemical network may survive and the chemical network keeps the stress for the most part in large deformation. In addition, according to Ghani et al., the volume resistivities of CB-filled rubber (natural rubber, SBR and isoprene rubber (IIR)) vulcanizates decreased after heat-treatment.[26] They presumed that the CB network of CB-filled rubber vulcanizates was thermally ruptured. However, it has never been reported to observe the rupture of the CB network directly. Therefore, in this study, the ruptured CB network of the CB-filled NR vulcanizate by heat-treatment under vacuum is observed directly by 3D-TEM, and the fraction of the network chains is analyzed by using a 3D image processing method that we have developed. The thermal change in the fractions of the CB network is also investigated on the basis of the volume resistivity.

Filler-filler and rubber-filler interactions

Six kinds of different fillers,[27] that is, carbon black, silica, clay, talc, mica, and titanium oxide are used in the rubber product such as the automobile tire. In these fillers, carbon black[28] and silica[29] are the most widely used. Because the rubber-filler and the filler-filler interactions occur in the filler-filled rubber, peculiar visco-elasticity phenomena such as the strain amplitude dependence of the complex dynamic moduli (Payne effect), thixotropic behavior, and frozen memory are experimentally observed.[30–35] For silica-filler rubber compounds, silica surface have hydrophilic siloxane and silanol groups, resulting in strong filler-filler interactions by hydrogen bonds and weaker van der Waals bonds.[36,37] As a result, dispersing silica in rubber compounds is much more difficult than carbon black dispersion. Silane coupling agents are used to improve the filler dispersion and to prevent adsorption of curatives on the silica surface, thus increasing the reinforcing effect to the rubber compounds.[38] The increase in concentration of fillers enables filler–filler interaction, which promotes the formation of filler agglomerates. For instance, $CaCO_3$ particles are generally supplied as agglomerates and during processing they are broken and dispersed into primary particles. Large particle–particle interactions result in inhomogeneous distribution of the filler, processing problems, poor appearance, and inferior properties. This fact may emphasize the importance of homogeneity where the increasing amount of aggregates leads to a decrease of tensile properties of the rubber composites.[39–42] When there is good interaction between the polymer matrix and filler, the opportunities for agglomeration will be less. Whereas, owing to the large surface energy for the nano-particles, when increase the amount of the filler–filler interaction will increase resulting in agglomerates.[42]

Conversely, it is believed that the rubber–filler affinity is their interaction including both physical and chemical absorption.[43] In other words, the strong interaction between polymers and fillers leads to the formation of rubber–filler junctions. Maier et al.[44] and Havet et al.[45] proposed a phenomenological model for the Payne effect based solely on the interaction between fillers and rubber chains. The properties of the rubber-filler interaction were further investigated by bound polymer measurements and by solid-state ^1H NMR experiments on the bound rubber fractions.[33,34,46,47] The mobility of the polymer segments immediately adjacent to the filler surface is significantly reduced, as evidenced by faster spin-spin relaxation. When the polymer–filler interactions dominate, it has shown experimentally that the nonlinear visco-elasticity of the suspension originates in the dynamics of the stick-slip motion of polymeric chains on and close to the filler surface.[45,48]

It is well known that bound rubber is produced in the mixing process of fillers (i.e., carbon black, silica, and etc.) and rubbers, and fillers are surrounded by bound rubber which consists of mainly two polymer phase of different molecular mobility.[33,34,46,47] Especially, carbon blacks disperse not as a separated particle but as an aggregate consist of 5–10 particles together in matrix rubber. It is believed that a

TABLE I
Recipes of Carbon Black-Filled NR Compounds[a]

Samples	CB-0	CB-5	CB-10	CB-20	CB-30	CB-40	CB-50	CB-60	CB-80
Ingredient (phr[b]): NR (RSS#1)	100	100	100	100	100	100	100	100	100
Stearic acid (ST)	2	2	2	2	2	2	2	2	2
Active ZnO	1	1	1	1	1	1	1	1	1
CBS[c]	1	1	1	1	1	1	1	1	1
Sulfur	1.5	1.5	1.5	1.5	1.5	1.5	1.5	1.5	1.5
Carbon black[d]	0	5	10	20	30	40	50	60	80

[a] Curing conditions: 140°C, 15 min under pressure.
[b] Parts Per 100 rubber by weight.
[c] *N*-cyclohexyl-2-benzothiazole sulfonamide.
[d] HAF grade, dried at 120°C for 2 h.

secondary network of polymer chains connecting filler particles forms.[49–52] This transient network is believed to be the cause of the large enhancement observed in visco-elastic properties. The transient network also produces a rubberlike behavior in a certain range of frequences.[50] Filler networking in elastomer composites can be analyzed by employing transmission electron microscopy (TEM) and dielectric measurements. TEM observation gives a limited microscopic of filler-network morphology. This is mainly due to the spatial interpenetration of neighboring flocculated filler clusters.[53] Flocculation studies, considering the small-strain mechanical response of the uncross-linked composites during heat treatment (annealing), demonstrate that a relative movement of the filler particles take place that depends on particle size, molecular mass of rubber, as well as rubber–filler and filler–filler interactions. This provides strong experimental evidence for a kinetic cluster–cluster aggregation (CCA) mechanism of the filler particles in the rubbery matrix to form a filler network.[54] From the dielectric investigations, it becomes obvious that charge transport above the percolation threshold is limited by hopping or tunneling mechanism of charge carriers over small gap of order 1 nm between carbon black particles.[55]

Recently, Fukahori[53] has proposed the new model has a double-layer structure of bound rubber, consisting of the inner polymer layer of the glassy state (grassy hard or GH layer) and the outer polymer layer (sticky hard or SH layer). Molecular mobility is strictly constrained in the GH layer and considerably constrained in the SH layer compared with unfilled rubber vulcanizate. The GH layer plays a role to fix several parts of a molecule in the SH layer to the surface of carbon particles. On the other side, the SH layer seems to be strongly adhered to the surrounding matrix rubber vulcanizate. It seems to be performed by chemical crosslinking or strong entanglement between molecules at the boundary surface of the SH layer and the matrix rubber. This means that the GH layer does not relate to the stress upturn at large extension, instead the SH layer must play a very important role at large extension.

Furthermore, in the case of strong filler–filler interactions, it is believed that the material response such as nonlinear visco-elasticity is greatly influenced by the evolution of the network of filler aggregates and its breakdown, rearrangement and reformation during mechanical and dynamic measurements.[30,31,33,56] On the other hand, when the rubber–filler interactions dominate, it has shown experimentally that the nonlinear visco-elasticity of the suspension originates in the dynamics of the stic-slip motion of polymeric chains on and close to the filler surface.[45,48,57] For example, increasing the amplitude of deformation beyond the linear visco-elastic region leads to a gradual breakdown of the filler network, manifested in a sharp decrease in dynamic storage modulus (G'). The cyclical nature of the deformation process also give rise to a dynamic loss modulus (G'') peak located in the amplitude range where the filler network is broken down but can still be restored quickly enough compared to the frequency of deformation.[30,58] From simulation of stress–strain cycles at medium and large strain it can be suggested that the model of cluster breakdown and reaggregation for prestrained samples represents a fundamental micromechanical basis for the description of nonlinear visco-elasticity of filler-reinforced rubbers. Thereby, the mechanisms of energy storage and dissipation are traced back to the elastic response of tender but fragile filler clusters.[54]

EXPERIMENTAL

Material: CB-filled NR vulcanizates

The compounding recipes of the CB-filled natural rubber (NR) vulcanizates investigated in this work are given in Table I. The only ingredient changed in this series of the CB-filled NR vulcanizates was the amount of CB loading, which was varied from 0 phr to 80 phr (parts per 100 rubber by weight). The

quantities of the other compounding agents were all the same; 2 phr of stearic acid, 1 phr each of active zinc oxide (ZnO) and *N*-cyclohexel-2-benzothiazole sulfenamide (CBS), and 1.5 phr of sulfur. Particle size of the ZnO were submicron in size (ca. 0.29 μm).[59] The Heat-Pressing Machine provided by Gonno Hydrulic Press Manufacturing CO. was employed as a vulcanization machine. Vulcanization was performed under pressure of ca. 10 MPa at 413 K for 15 min in a compression mold.

We have previously described the 3D skeletonized network structure of the CB aggregates in natural rubber vulcanizates.[17–21] It was found that independent CB aggregates were present locally at a low CB loading below 20 phr, whereas at CB loadings above 30 phr, the CB network was extended throughout the entire sample. To estimate a change in the CB network structure, CB-filled NR vulcanizates at CB loadings above 30 phr are to be used. Therefore, To investigate thermal destruction of the CB network structure, 50 and 80 phr CB-filled NR vulcanizates (CB-50 and CB-80) were chosen this time for 3D-TEM measurements.

APPARATUS AND PROCEDURE

Heat-treatment

To the most suitable heat-treatment temperature, we employed DSC measurements of CB-filled NR vulcanizates at first. From the DSC results, it is clarified that the thermal decomposition temperature (exothermic peak temperature) of the matrix rubber is 470 K. The heat-treatment temperature should be selected lower temperature than this thermal decomposition temperature. Next, the visco-elastic behavior, that is, the temperature dependence of tan δ, was noted. With increase of the temperature, tan δ of CB-0 and CB-10 decreased approximately linearly. In contrast, with CB loading more than 20 phr, the temperature dependence of tan δ tends to become convex up. In particular, the clear peak of tan δ is observed at about 383 K in CB-50, CB-60, and CB-80. From these facts, it is thought that this peak is attributed to a change of CB aggregate and CB network in rubber matrix.

Conversely, the temperature dependence of the thermal expansion in the nitrogen atmosphere increases linearly with an increase in temperature at the temperature lower than 390 K, whereas the temperature dependence deviates from the approximately linear line of the lower temperature at the temperature higher than 390 K. Especially, the temperature tendencies of CB-0 and CB-10 have a peak at the temperature higher than 390 K. These deviations and peaks suggest that because the radicals generated by the thermal degradation of rubber molecular chains are recombined, the network-chain density of rubber matrix increases in the nitrogen atmosphere, and the thermal expansion is reduced at the temperature higher than 390 K. From these results, it is concluded that the most suitable heat-treatment temperature, which minimizes thermal degradation of the rubber matrix and causes the most efficient structural change of CB aggregates and CB network, is 383 K. However, it was experimentally difficult to heat-treatment a large number of samples in the nitrogen atmosphere. Therefore, it was thought that the heat-treatment effect was achieved by the heat-treatment in a vacuum. The samples were placed in a vacuum oven (DP33 provided by Yamato Scientific Co., Ltd.) kept at 383K for a specified period of time. The heat-treated samples were then removed from the oven followed by their cooling to room temperature (R.T.). A small amount of oxygen might remain in the oven chamber because the vacuum level that reached with a rotary vacuum pump was about 4 kPa (30 Torr).

Characterization of network-chain density of rubber matrix

Network-chain density of rubber matrix (ν) of CB-filled NR vulcanizate was determined by the swelling method in benzene at 303 K. The original weight of a dry sample and that of a swollen sample to the equilibrium were measured with a balance. In the swelling of CB-filled NR vulcanizates, benzene was used as a solvent. In this case, the interaction coefficient (χ) between NR vulcanizate and benzene is 0.380 at 303 K (30°C).[60] Network-chain density of the rubbery matrix was calculated from these volume fractions by using the Flory-Rehner's equation[61] taking the weights of CB and ZnO that are not swellable into account.

On the other hand, because that the particle size of active zinc oxide is much smaller than that of a general zinc oxide, active zinc oxide is more excellent in dispersion to rubber, and has higher surface-activity than a general zinc oxide. Therefore, it is thought that active zinc oxide efficiently promotes the vulcanization reaction compared with a general zinc oxide. In fact, NR vulcanizates (CB-50 and CB-80) crosskinked with active zinc oxide 1 phr, are not dissolved in an organic solvent such as benzene, and imply an ordinal mechanical property. Additionally, from the swelling method, the network-chain densities of CB-50 and CB-80 are 0.17 and 0.24 mol/dm,[3] respectively. Therefore, we believe that the amount of active zinc oxide to promote the vulcanization reaction of natural rubber is enough by 1 phr.

Measurement of thermal behavior

To investigate the most appropriate and effective heat-treatment temperature for CB-filled NR

vulcanizate without thermal degradation in the N_2 atmosphere, the Differential scanning calorimetry (DSC) measurements were carried out. During heat-treatment under this temperature, it are thought that destruction and rearrangement of CB network are caused without thermal degradation of the rubber matrix.

The DSC mesurement was examined by using a TA Instrument DSC-Q1000 equipment with increasing temperature at rate of 10 K/min from 173 K to 523 K in N_2 gas atmosphere. Glass transition temperature (T_g) and thermal decomposition temperature (T_d) were detected during by the heating process.

Measurement of dynamic visco-elasticity

Storage modulus (E') and tangent loss (tan δ) under the tensile mode at 20 Hz, were measured by using a Rheometric Scientific RSA II equipment with increasing temperature at rate of 2 K/min from 293 K to 393 K in N_2 gas atmosphere. The size of specimen was 5 mm width, 35 mm length and 1 mm thickness.

Measurement of thermal expansion

Thermal expansion under tensile mode loading of 0.098 N, was examined by using a Seiko Instrument TMA120C equipment with increasing temperature at rate of 2 K/min from 273 K to 423 K in N_2 gas atmosphere. The size of original specimen was 3 mm width, 15 mm length and 1 mm thickness.

Measurement of volume resistivity

The volume resistivity of the samples was measured with the three-electrode method using an R8340A ultra-high resistance meter (Advantest Corp.) with a main electrode (stainless steel; 50-mm dia.), a guard electrode (stainless steel; internal/external dia. of 70/80 mm) and a counter electrode (stainless steel; 103-mmdia.). A sheet-shaped NR vulcanizate sample was tightly sandwiched between the main and guard electrodes and the counter electrode. The guard electrode was grounded to prevent current from flowing along the sample surface. The applied voltage was 100 V or 1 V. The volume resistivity was calculated from the current that flowed through the sample when a certain specified voltage was applied. This measurement method conforms to the procedure specified in the relevant Japanese Industrial Standard (JIS K 6911, which is equivalent to ISO D-257-90, "Standard Test Method for DC Resistance on Insulating Materials"). Sample cells were also loaded in a constant-temperature bath (TR-43C provided by Advantest Corp.) that was used to keep the temperature at 296K (23°C) during the measurement.

TEM and 3D-TEM observations

As was pointed out by Coran,[62,63] ZnO reacts with sulfur and/or the vulcanization accelerators such as CBS (*N*-cyclohexyl-2-benzothiazole sulfenamide) in the sulfur vulcanizing process to produce rubber-soluble Zn compounds. Because such Zn compounds cause the electron beam to scatter, clear TEM and 3D-TEM images were not obtained in preliminary studies when thin specimens simply cut from the sulfur-cured NR were used. To avoid this problem, two original pretreatment processes were applied to the NR vulcanizates used in this study to obtain suitable samples for TEM and 3D-TEM observations. In one process, the NISSAN ARC-AK method[17–21,64–67] was used to remove rubber-soluble Zn compounds that cause the electron beam to scatter. An ultra-microtome was used to cut thin specimens from the pretreated NR vulcanizates that had been frozen at the temperature of liquid nitrogen (75 K). The NISSAN ARC-SG method[17–21,64–67] was then applied as the second pretreatment process to make the thickness of the thin specimens uniform and simultaneously to smooth their surface. The samples thus obtained for TEM and 3D-TEM observations were ~ 600 nm long, ca. 600 nm wide, and ca. 200 nm thick.

The instruments used in the conventional TEM and 3D-TEM observations were a H800 (HITACHI Company) and a Tecnai G2 F20 (FEI Company), respectively, with the accelerating voltage of the electron beam set at 200 kV. Especially, the 3D-TEM observation procedure is schematically in shown Figure 1. Samples were tilted in a range of angles from −70° to + 70°, and image data (tilted images) were obtained sequentially in 2° steps. Specifically, a series of 71 sequential tilted images in total were input into a computer. It is well known that organic polymers are susceptible to damage by an electron beam,[68,69] which is an issue that must always be considered in 3D-TEM observations.[17–21,63–66] Using the IMOD program[70] (software developed at the University of Colorado) installed on the Tecnai TEM, the sequential series of tilted images were converted to image slices showing the mass-density distribution of the sample at each angle. The AMIRA program[71] (developed by TGS Co.) was then used to reconstruct 3D images from the image slices. Additionally, in the conventional TEM image, the nanofiller is observed only in two dimensions on a nanometer scale. Since the morphology in the thickness direction of the sample is only obtained as an accumulated one in this two-dimensional image, it is practically impossible to recognize the aggregation of the nanofiller in the thickness direction. In contrast, with 3D-TEM, we can obtain such information in the direction of the sample thickness. In this study, we set the thickness of the samples at about

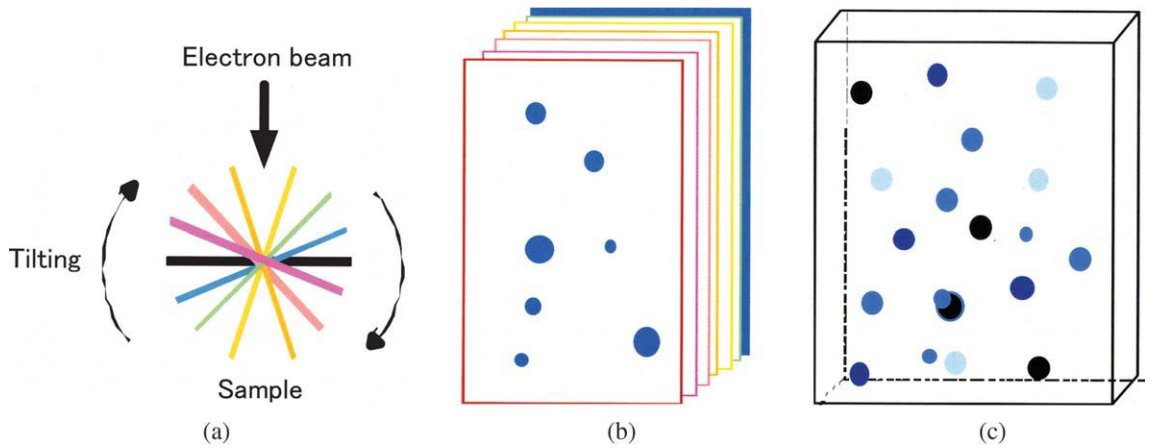

Figure 1 Observation principle and conditions of 3D-TEM. Performed Radon transform operations on the image slices to construct 3D images. (a) Tilting sample (ca. 600 × 600 × 200 nm):Single axial tilting from −70°to + 70°in 2°steps. (b) 2D projections: sequential image slices. (c) Reconstructed 3D image. [Color figure can be viewed in the online issue, which is available at wileyonlinelibrary.com.]

200 nm so that the electron beam could penetrate them easily.

RESULTS AND DISCUSSION

Thermal behavior of CB-filled NR vulcanizates

Temperature dependence of heat flow (HF) of CB-filled NR vulcanizate is indicated in Figure 2. Glass transition temperature (T_g) appeared at about 210 K. HF decreases with increasing temperature above T_g and is saturated at ca. 420 K. Thermal decomposition occurs at about 470 K in the nitrogen atmosphere. It is thought that a little thermal oxidation reaction[72] of sulfur-cured NR may occur at our heat-treatment conditions (i.e., 383 K under vacuum) employed in this study. In addition, the HF of the CB-filled NR vulcanizate is higher than that of the unfilled one (CB-0) before the thermal decomposition temperature. This fact means that the thermal capacity and/or thermal conduction of CB-filled NR vulcanizates are clearly different from CB-0.

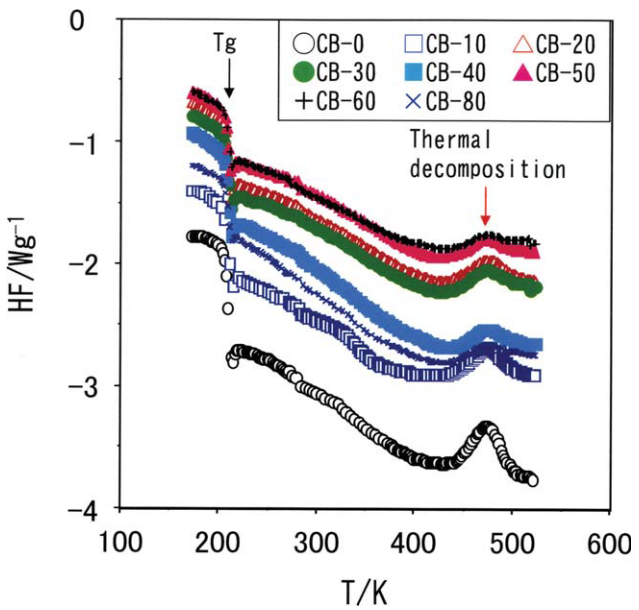

Figure 2 Results of DSC measurements: Temperature dependence of heat flow (HF) of CB-filled natural rubber (NR) vulcanizates in nitrogen atmosphere. [Color figure can be viewed in the online issue, which is available at wileyonlinelibrary.com.]

Dynamic visco-elasticity

It is known that a structural change of CB-filled NR vulcanizate is reflected in the dynamic visco-elastic behavior.[73–75] For example, physical interaction between rubber molecular chains and CB is assumed to be the origin of the Payne effect,[73] which is related to the dependence of dynamic modulus of filled rubbers on frequency amplitude. According to McDonald et al.,[74] E′ tends to increase with increases of loading, specific surface area, surface activity and unit size of distribution of CB in rubbery matrix. They believed that this tendency was closely related to the change of CB-gel dispersion structure. For resilience, the most important CB variables appear to be CB loading, unit size, unit size distribution, surface activity, and structure. In addition, Kraus[75] reported that tan δ of CB-filled butyl rubber vulcanizate increased by increasing CB loading before the forming of CB network structure and remained almost constant after the formation. Perhaps, the above-mentioned increase of E' may be attributable to CB network structure rather than CB primary structure.

Figure 3 indicates the temperature (T) dependence of dynamic mechanical properties, namely storage modulus (E') and loss tangent (tan δ), of CB-filled NR vulcanizates. E' of CB-filled NR vulcanizate decreases by increasing T and is saturated over the temperature higher than 380 K. Additionally, reduction of E'

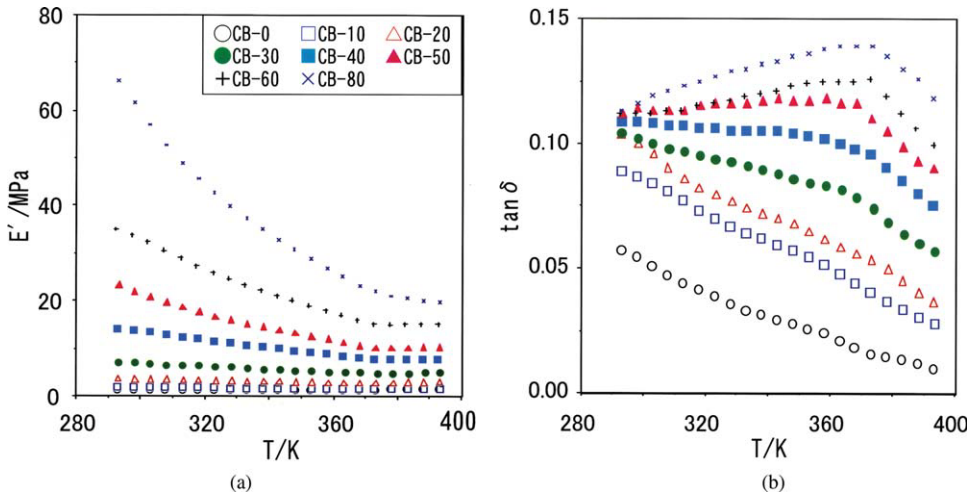

Figure 3 Temperature (T) dependence of dynamic mechanical properties of CB-filled NR vulcanizates in nitrogen atmosphere. (a) Storage modulus (E'). (b) Loss tangent (tanδ). [Color figure can be viewed in the online issue, which is available at wileyonlinelibrary.com.]

increases with increase of CB loading. It is suggested that this reduction is related to a decrease of interaction between rubber molecular chains and CB. On the other hand, tan δ increases with an increase of CB loading. This fact means that amount of the interaction between rubber molecular chains and CB becomes larger by increasing CB loading. Interestingly, the temperature dependence of tan δ on CB loading changes remarkably and uniquely by the CB loading. The tan δ decreases with an increase of temperature almost linearly at CB loading less than 20 phr. The temperature dependence of tan δ curves over 30 phr shows a tendency to give a maximum value, clearly to give it at CB-50, 60, and 80. The maximum peak of tan δ of CB-80 appears at ~ 380 K. Therefore, it is thought that after the interaction such as the bound rubber layer around the CB aggregate in the CB network is lost at about 380 K, rearrangement of CB aggregates and/or destruction of CB network structure occur at this temperature or higher.

Rivin et al.[76] reported that from a model experimental result about adsorption of 2-methyl-2-octene to CB, 95% of the CB surface area was adhesion by van der Waals forces, and that the remaining 5% surface area was chemical combination. In addition, the most of bound rubber of CB- and silica-filled SBR/BR compound dissolved in chloroform after supersonic wave irradiation.[77] This suggests whether a small amount of crosslinking points exist in bound rubber, or any crosslinking points does not exist in it. From these facts, it is thought that the most of the quantity of bound rubber is formed by a physical interaction between matrix rubber and inorganic filler such as CB. On the other hand, according to Printer et al.,[78] the bound rubber of CB-filled SBR begins to reduce over 373 K (60°C), and disappears mostly at about 423 K (150°C). According to Pérez et al.,[79] the results of MTDDSC (Modulated Temperature Differential Scanning Calorimetry) measurements, revealed that the thermal behavior of the bound rubber of CB- and silica-filled SBR/NBR, was reversible in the temperature region from the room temperature to 423 K (150°C). Considering the above-mentioned results, bound rubber which is containing CB aggregates and CB network, disappears mostly or partially in a higher temperature. It is believed that CB aggregates and CB network are destructed and their fragments are rearranged after reduction and disappearance of bound rubber. Moreover, during cooling, bound rubber is reproduced reversibly in the inside and outside of the CB aggregates and CB network.

Thermal expansion

The thermal expansion is one of the general and basic characteristics, and in the case of rubber products it depends on network-chain density of rubber, CB loading in rubber, and so on. Temperature (T) dependence of thermal expansion (L) of CB-filled NR vulcanizate is indicated in Figure 4. L is defined as follows.

$$L = 100 \cdot \left(L_T \Big/ L_{RT} \right) \tag{1}$$

L_T: Sample length at an arbitrary temperature (T)
L_{RT}: Sample length at room temperature

L increased with T almost linearly up to ~ 380 K, and decreased with CB-loading. Since thermal expansion of CB is much smaller than the rubbery matrix, the result is reasonable. Especially, behavior of CB loading more than 20 phr is different from that of CB loading less than 20 phr in term of L. This difference

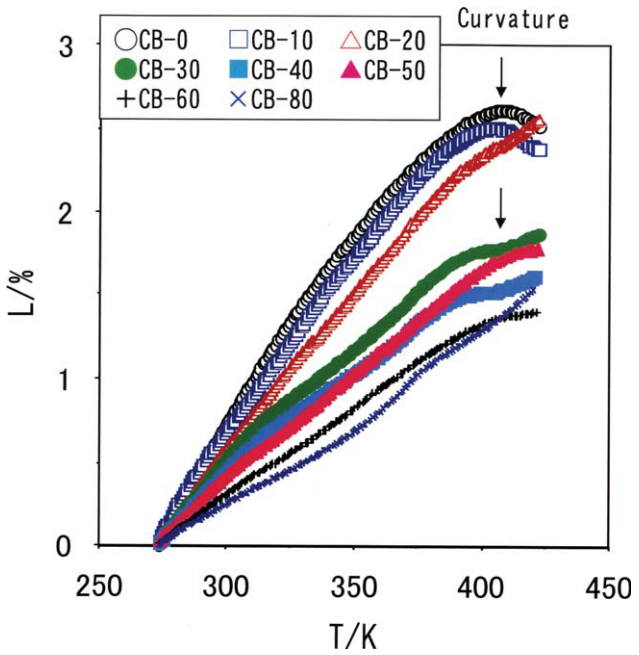

Figure 4 Temperature (T) dependence of thermal expansion (L) of CB-filled NR vulcanizates in nitrogen atmosphere. [Color figure can be viewed in the online issue, which is available at wileyonlinelibrary.com.]

at 20 phr may be due to the fact that these may be a critical point of formation of CB network in rubbery matrix between the CB loadings of 20 phr and 30 phr. In fact, we have reported that CB network structure in CB-filled NR is formed at the CB loading more than 20 phr, which is elucidated by 3D-TEM techniques.[17–21] In addition, temperature dependence of L curves seem to give maximum at a temperature higher than ca. 400 K. Taking into account the thermal decomposition temperature in Figure 2, this curvature might be due to the occurrence of rearrangement of CB aggregates and/or thermal destruction of CB network structure. From these results, 383 K was selected as the heat-treatment temperature for investigating thermal destruction of CB network structure, hopefully without thermal decomposition of rubber. In addition, a vacuum condition was employed in the heat-treatment of the samples instead of the N_2 gas atmosphere. However, it was thought that a thermal oxidation reaction by the remaining oxygen was not completely avoided.

The behavior of the thermal expansion of CB 20 phr loaded sample (CB-20) is different from the other samples. In other words, the temperature dependence of thermal expansion of CB-20 is similar to CB-0 and CB-10, while this dependence does not have a peak at high temperatures. In addition, the thermal expansion behavior of CB-20 is markedly larger than those of the samples loaded more than 30 phr. To clarify these differences, we think that it is necessary to investigate about the relationship between thermal expansion behavior and CB dispersion structure in the future study. On the other hand, the deviation from linear thermal behavior and the peak of the behavior in the higher temperature region are focused on this time. We have investigated the relationship between the electric properties and CB dispersion structure of CB-filled NR vulcanizates by using the measurements of the volume resistivity, dielectric measurements and 3D-TEM observation.[19] It is found that the electric properties of the samples loaded CB 10 phr or less are remarkably different from the samples loaded CB 30 phr or more. Furthermore, 3D-TEM observation reveals that CB aggregates are locally dispersing in the rubber matrix in the region of CB loading of 10 phr or less, whereas CB network is formed in the region of 30 phr or more. CB-20 shows the intermediate behavior and morphology between them. It is thought that thus characteristics of CB-20 are closely related to its thermal expansion behavior.

As mentioned above, the temperature dependence (Fig. 4) of the thermal expansion increases linearly with an increase in temperature at the temperature lower than 390 K, whereas, the temperature dependence deviates from the approximately linear line of the lower temperature at the temperature higher than 390 K. Especially, the temperature tendencies of CB-0 and CB-10 have a peak at the temperature higher than 390 K. This deviation suggests that because the radicals generated by the thermal degradation of rubber molecular chains are recombined, the network-chain density of rubber matrix increases, and the thermal expansion is reduced at the temperature higher than 390 K. Therefore, we selected 383 K as the heat-treatment temperature to avoid from thermal degradation of the rubber matrix.

Dependence of volume resistivity (ρ_v) on heat-treatment

It has been reported that the volume resistivity (ρ_v) of CB-filled NR vulcanizates decreased sharply with a higher CB loading up to 30 phr, at which it declined only gradually and tended to converge to a constant level above 40 phr.[17,19,20] In the low CB loading region, it is assumed that electron hopping is assisted by conductive impurities (maybe, ionic ones), located in close proximity due to the thermal segmental and/or the whole motion of the rubber molecular chains. In contrast, in the high CB loading region, an electron conductive path having a CB network structure is formed, through which electrons move more easily. Based on these backgrounds, the effect of the heat-treatment conditions on ρ_v is examined in this study.

Figure 5 shows the dependence on the heating time (T_h) for CB-0, CB-5, CB-10, CB-50, and CB-80 at

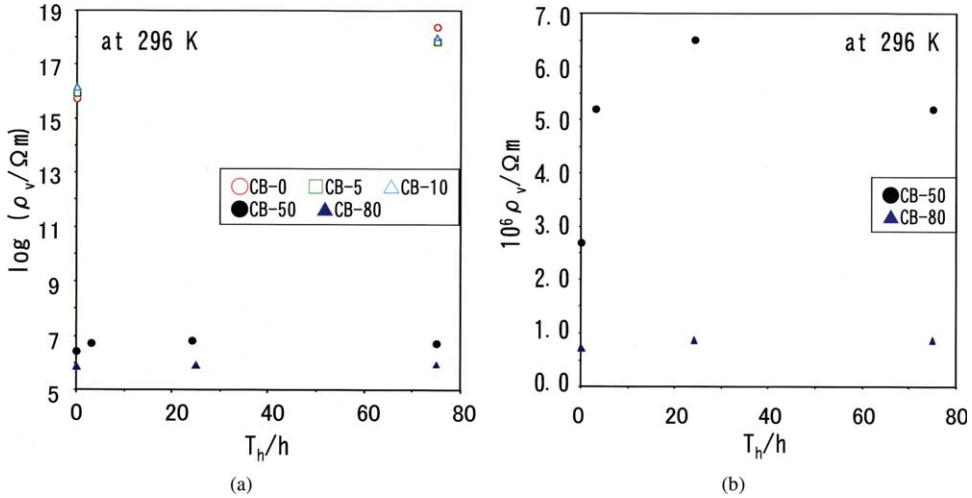

Figure 5 Dependence of volume resistivity (ρ_v) of CB-filled NR vulcanizates on heat treatment time (T_h) at 383 K in vacuum. (a) CB-0, 5, 10, 50, and 80. (b) CB-50 and 80. [Color figure can be viewed in the online issue, which is available at wileyonlinelibrary.com.]

383 K under vacuum. CB-0, CB-5 and CB-10 are the reference samples. In Figure 5(a), it is shown that the ρ_vs of CB-0, CB-5 and CB-10 are significantly higher than those of CB-50 and CB-80. In other words, CB-50 and CB-80 are much more electron-conductive than the others. Furthermore, Figure 5(b) shows that the ρ_v of CB-50 increased rapidly up to a heat-treatment time of 24 h and it decreased by further heat-treatment, whereas the ρ_v of CB-80 remained almost constant without depending on heating time. Ghosh et al.[80] have reported that the conductivity (reciprocal of ρ_v) of CB-filled cured EPDM increased nonlinearly with temperature in the region from 296 K to 473 K. They noted that electrons probably easily jumped between CB aggregates because the energy barrier was lowered by the thermal motion of CB accompanying with that of the rubbery matrix by increasing temperature. Additionally, Kimura et al.[81] have reported that the ρ_v of 40–60 phr CB-filled SBR decreased with an increase of heat-treatment time and that of temperature, respectively. They thought that the scission of rubber molecular chains introduced some functional groups in the rubber due to a thermal oxidation reaction, by which the conductivity increased. Their results do not agree with ours shown in Figure 6. It is thought that our heat-treatment has presumably induced not only thermal degradation of rubbery matrix but also some changes in the CB network structure. The thermal degradation is examined by the change in the network-chain density which is described latter.

On the other hand, Mohanraj et al.[82] have suggested that the ρ_v of CB-filled NR vulcanizates increased with an increase of temperature. They thought that this increase of ρ_v was closely related to the change of the CB dispersion structure in the rubbery matrix. However, they did not give any direct proof of the occurrence of such structural change. Therefore, we used 3D-TEM observation technique as well as the volume resistivity measurement to investigate the CB structural change in CB-50 and CB-80 by the heat-treatment for 3 h or more at 383 K.

Network-chain density of rubber

Dependence of network-chain density (ν) of the rubbery matrix in CB loading of CB-filled NR vulcanizate before/after the heat-treatment at 383 K for 75 h is indicated in Figure 6 and Table II. The ν increases with an increase of CB loading. And, the

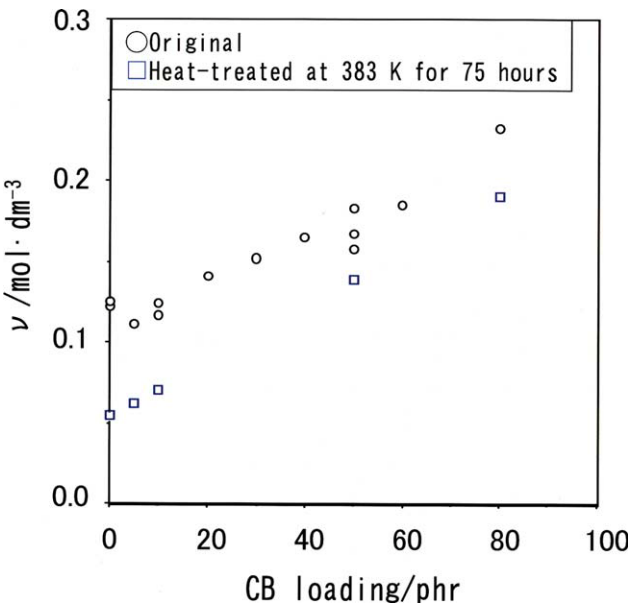

Figure 6 Dependence of network-chain density (ν) on CB loading of CB-filled NR vulcanizates before/after heat-treatment at 383 K for 75 h in vacuum.

ν of the heat-treated sample is lower than that of the original one. These results reveal that CB loading apparently increases ν and the heat-treatment decrease it. The former may be attributable to increase of CB total surface by increasing CB loading. The surface of CB is active to strongly absorb the rubber chains.[1,4,8,17] The latter suggests that the heat-treatment causes a thermal oxidation reaction with chain-scission of rubber molecular and slightly generates functional groups which reduce the ρ_v. However, it is difficult to explain the dynamic mechanical properties in Figure 3 by these ν's before/after the heat-treatment, because that the reduction ratio of ν after the heat-treatment decreases with increasing in CB loading. Of course, it seems that the heat-treatment time of Figure 3 is too short to reach the same time (75 h) as that of Figure 6 and Table II.

Taking into account the results of the DSC, the dynamic mechanical and the thermal expansion measurements of CB-filled NR vulcanizates, we selected the most suitable heat-treatment temperature, which minimizes thermal degradation of the rubber matrix and causes the most efficient structural change of CB aggregates and CB network, is 383 K. These measurements were carried out in the nitrogen atmosphere. However, a large amount of heat-treatment sample is needed for various analyses and measurements. Accordingly, the samples were heat-treated in the vacuum oven. The vacuum level at this time was $\sim$ 4 kPa (30 Torr), and a small amount of oxygen remained in the oven. As a result, it is thought that the heat oxidation deterioration happens a little, and the network-chain density (ν) of the heat-treatment sample decreased a little compared with the virgin sample as shown in Figure 6 and Table II. On the other hand, because the experiment by Kimura et al.,[81] was carried out in air, the network-chain density of their samples after oxidation degradation is remarkably lower than our samples.

TABLE II
Dependence of Network-Chain Density (ν) on CB Loading of CB-Filled NR Vulcanizates Before/After Heat-Treatment at 383 K for 75 h

CB loading/phr	ν/mol dm^3
(a) Samples before heat-treatment[a]	
0	0.121
0	0.124
5	0.111
10	0.117
10	0.124
20	0.141
30	0.152
40	0.165
50	0.158
50	0.167
50	0.183
60	0.186
80	0.233
(b) Samples after heat-treatment	
0	0.0549
5	0.0621
10	0.0706
20	–
30	–
40	–
50	0.139
60	–
80	0.191

[a] Original sample

TEM and 3D-TEM observations of heat-treated samples

Figures 7 and 8 show the TEM images of CB-filled NR vulcanizates (CB-50 and CB-80) into the manuscript. The black particles observed in the TEM images, are carbon blacks. The images indicate that the heat-treatment destroys CB network and induces rearrangement of the network. Although, in the TEM images the detailed information about the depth profile disturbs to recognize the morphology changes of CB aggregate network before/after heat-treatment, quantitatively. Therefore, we have employed 3D-TEM observation of CB-filled NR valcanizates.

Figures 9 and 10 show 3D-TEM images of the CB aggregates of CB-50 and CB-80. One of the two samples was not heat-treated (a) and the other was heat treated at 383K for 75 h under vacuum (b). In Figures 9 and 10, their images can be constructed and displayed in black and white. CB aggregates appear as white forms in the images. There are the scale bars of 100 nm under the images on the right sides. Adjacent aggregates away from about 1 nm that is the resolution of 3D-TEM, are shown in these images so that they can be distinguished. These images show that the distribution of the CB aggregates and the CB network were changed before/after the heat-treatment. Concretely, compared with the images [(a) in Figs. 9 and 10] of CB-50 and CB-80 before the heat-treatment, the CB aggregates and the CB networks in the images [(b) in Figs. 9 and 10] show remarkable heterogeneity. From the 3D-TEM images, we calculated two distances between the aggregates. One is the closest distance (d_g) between the centers of gravity of two neighboring CB aggregates.[17–21] The other is the closest distance (d_p) between the two neighboring CB aggregates measured on a line between their centers of gravity. The two distances are shown in Figure 11. According to Kato et al.,[19] the closest distance (d_p) between CB aggregates is approximately 3 nm, the value at which volume resistivity (ρ_v) and the closest distance between CB

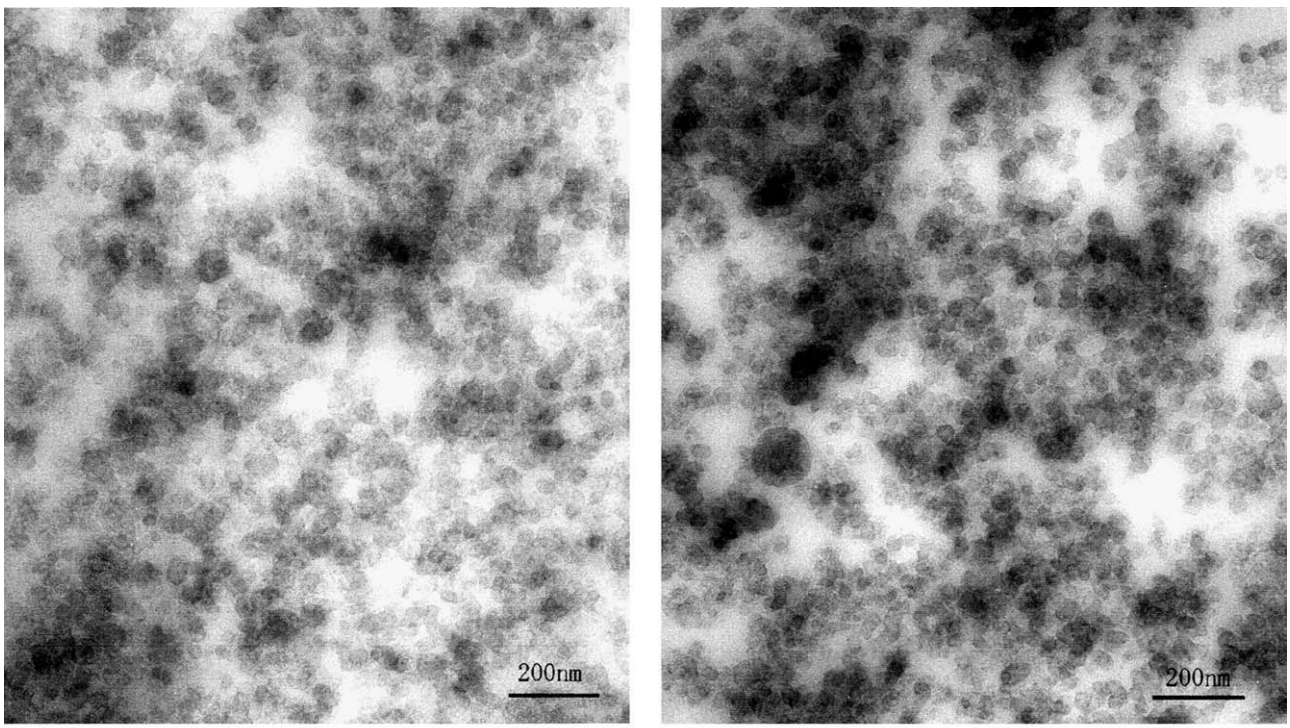

Figure 7 TEM images of CB-50 before/after heat-treatment at 383 K for 75 h in vacuum. (a) Before heat-treatment. (b) After heat-treatment.

aggregates were found to saturate in the high CB loading region. The equivalent sphere radius (R_E) of CB aggregates was approximately 30 nm in all of samples before/after the heat treatment. And, the d_p (ca. 3 nm) of the original samples are approximately the same as the values of the heat-treated ones.

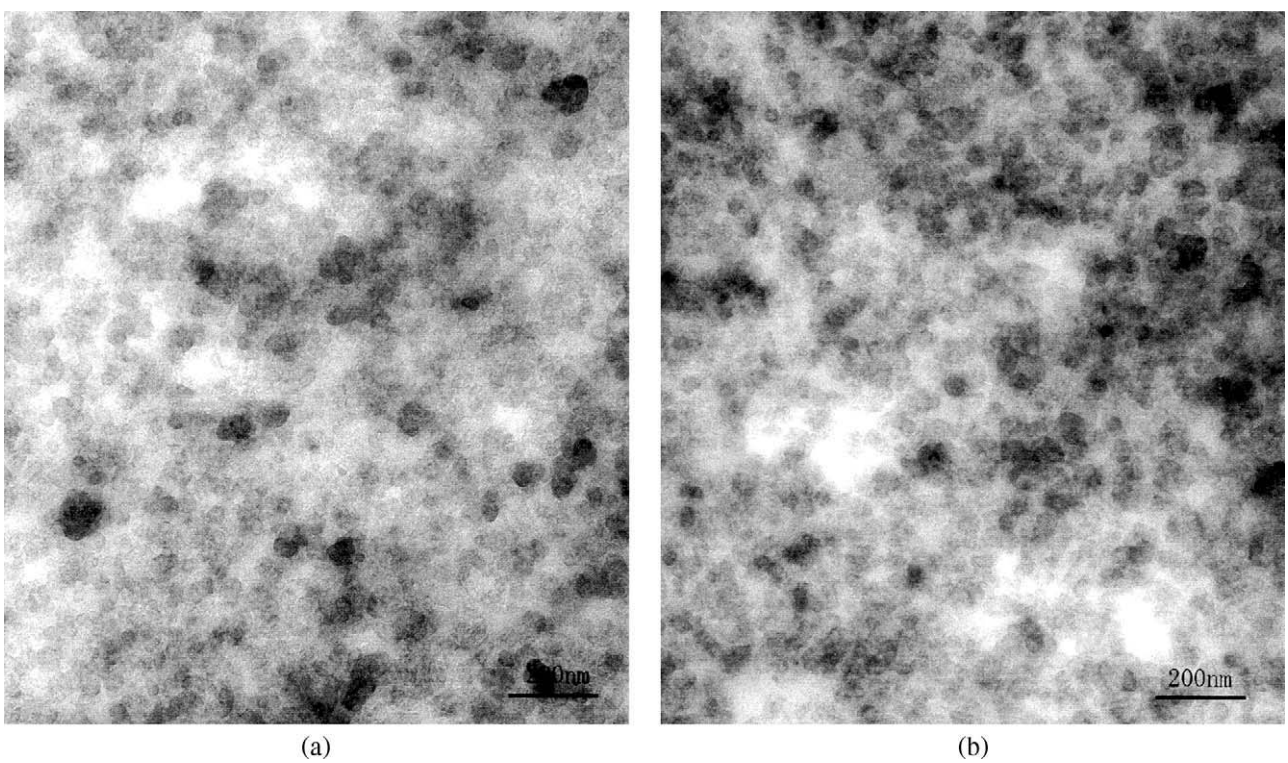

Figure 8 TEM images of CB-80 before/after heat-treatment at 383 K for 75 h in vacuum. (a) Before heat-treatment. (b) After heat-treatment.

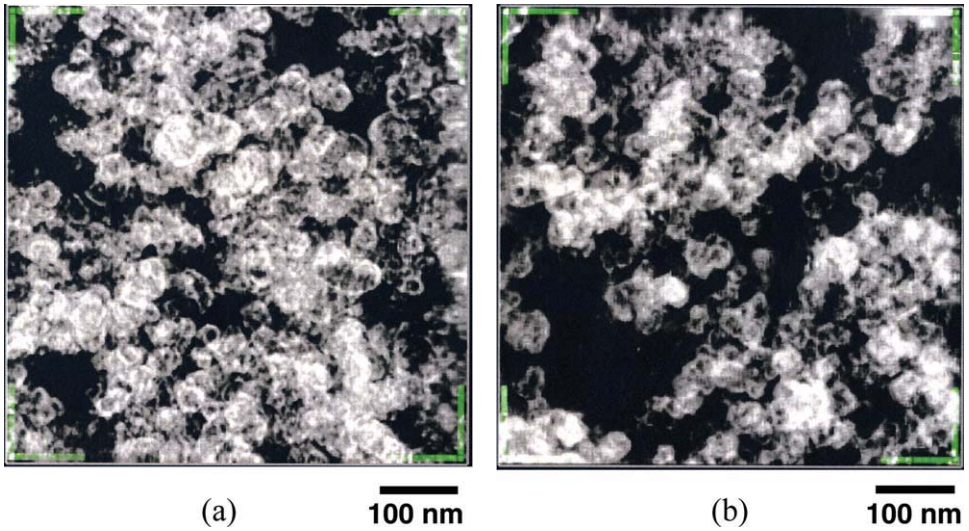

Figure 9 3D-images of original CB-50 and heat-treated CB-50 at 383 K for 75 h in vacuum. (a) Original. (b) Heat-treated. [Color figure can be viewed in the online issue, which is available at wileyonlinelibrary.com.]

Connecting the centers of gravity of neighboring CB aggregates separated by 3 nm or less resulted in a skeletonized representation of the network structure in the rubbery matrix.[18,19] The procedure is as follows. First, in the 3D-TEM image the center of gravity of each aggregate is positioned. Second, when the neighboring aggregates the d_p of which is equal or less than 3 nm are found, connect their centers of gravity by a line; i.e., the d_g is represented as a line. Third, continue the connection to all possible pairs. Last, only the lines are shown to result in the skeleton that shows the electron-conductive path.[17,19] Diagrams of the 3D skeletonized network structure of the CB aggregates in the original and the heat-treated samples (CB-50 and CB-80) are shown in Figures 12 and 13. It seemed that the CB network structure extended throughout the entire sample in the original CB-50 and CB-80, whereas the CB network in the heat-treated samples was markedly ruptured. Especially, thermal destruction of CB network structure is more remarkable in CB-50 than that in CB-80. The three-dimensional network structure formed by the clustering of the CB aggregates is schematically shown in Figure 14 together with the parameters of the network structures. The circles in this figure represent CB aggregates. The thin arrows indicate that the CB aggregate chains composed of a few aggregates are linked to the surrounding network structures. The two thick arrows show the crosslinking point (N_d) and the branching point (T_m)

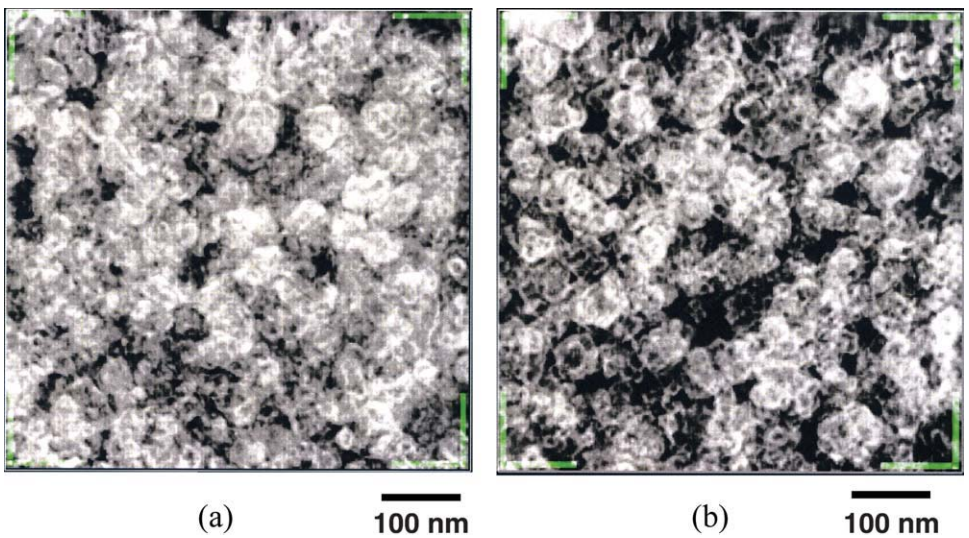

Figure 10 3D-images of original CB-80 and heat-treated CB-80 at 383 K for 75 h in vacuum. (a) Original. (b) Heat-treated. [Color figure can be viewed in the online issue, which is available at wileyonlinelibrary.com.]

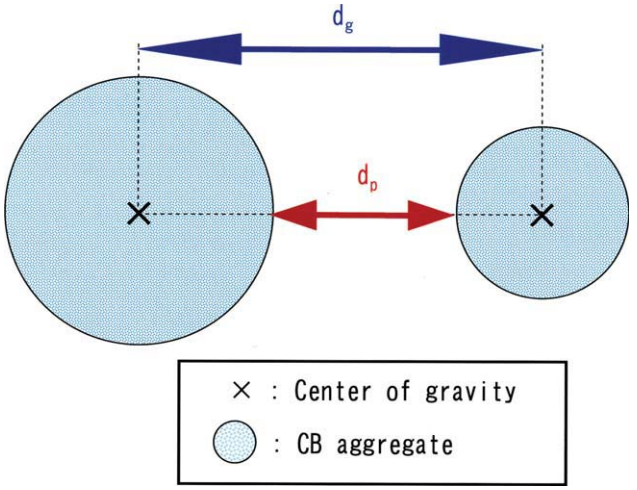

Figure 11 Definitions of the closest distance (d_p) between two neighboring aggregates and the closest distance (d_g) between the center of gravity of two neighboring aggregates as 3D parameters. [Color figure can be viewed in the online issue, which is available at wileyonlinelibrary.com.]

of the network, respectively. The length (L_{cross}) of the crosslinked chain is defined as the length between two crosslinked points and the length (L_{branch}) of the branched chain is defined as the length from the branched point to the end of the branched chain. The isolated chains which were independent of the network could not be found before/after the heat-treatment. The densities (D_{cross} and D_{branch}) of the crosslinked points and the branched points are defined as follows.

$$D_{cross} = N.Nd/TV \quad (2)$$

$$D_{branch} = N.Tm/TV \quad (3)$$

where $N.N_d$ is the number of the crosslinked points, $N.T_m$ is the number of the branched points, and TV: is the total volume containing the CB network. Next, the fraction of the crosslinked chains (F_{cross}) and the fraction of the branched chains (F_{branch}) are defined by the following equations.[19]

$$F_{cross} = N.NdNd/(N.NdNd + N.NdTm) \quad (4)$$

$$F_{branch} = N.NdTm/(N.NdNd + N.NdTm) \quad (5)$$

where $N.N_dN_d$ is the number of crosslinked chains, $N.N_dT_m$ is the number of the branched chains, and $N.N_dN_d$+$N.N_dT_m$ is the total number of the network chains. The two fractions (4) and (5) are the parameters to characterize the CB network structure.

It can be expected that this three-dimensional CB network structure formed by clustering of the CB aggregates is also closely related to various properties, in addition to electrical characteristics. It is noted that the crosslinked chains and the branched chains of the CB network were observed in CB-50 and CB-80 before/after the treatment examined. Table III shows the characteristics on the CB network structures of CB-50 and CB-80 before/after the heat-treatment (i.e., original samples and heat-treated ones at 383 K for 75 h in vacuum) obtained from 3D-images analysis of 3D-TEM images. This Table indicated the average lengths (L_{cross} and L_{branch}), D_{cross} and D_{branch}, and F_{cross} and F_{branch} of CB-50 and 80 before/after the heat-treatment. Compared with the original nonheated samples, the average lengths and D_{cross} of the heat-treated samples decreased, and D_{branch} increased with decrease of D_{cross}. These results reveal that the CB networks of CB-50 and CB-80 were broken and were rearranged by the heat-treatment. In addition, after the heat-treatment, F_{cross}'s of CB-50 and CB-80 decreased, whereas their F_{branch}'s increased. These suggest that the heat-treatment changed the composition of their CB networks. Especially, F_{branch} of CB-50 became larger than that of CB-80, while the decrease of F_{cross} of CB-50 was almost the same as that of CB-80 by the heat-treatment. And, F_{cross} and F_{branch} of the heat-treated CB-50 were the same compositions (F_{cross} and F_{branch} = ca. 0.7 and ca. 0.3, respectively) as those of the heat-treated CB-80. It is suggested that the CB network of CB-80 is more thermal stable

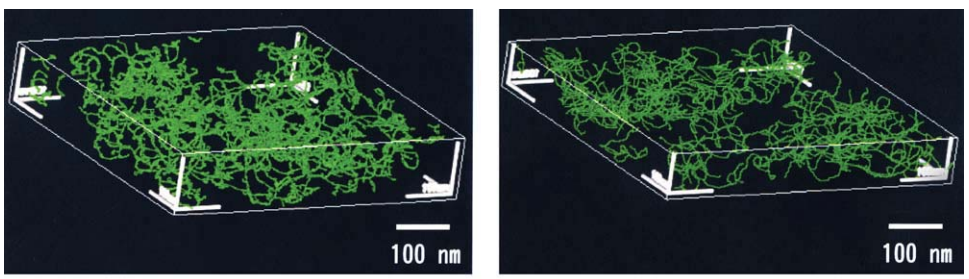

Figure 12 3D-TEM image analysis results for CB network of original CB-50 and heat-treated CB-50 at 383 K for 75 h in vacuum. (a) Original (b) Heat-treated. [Color figure can be viewed in the online issue, which is available at wileyonlinelibrary.com.]

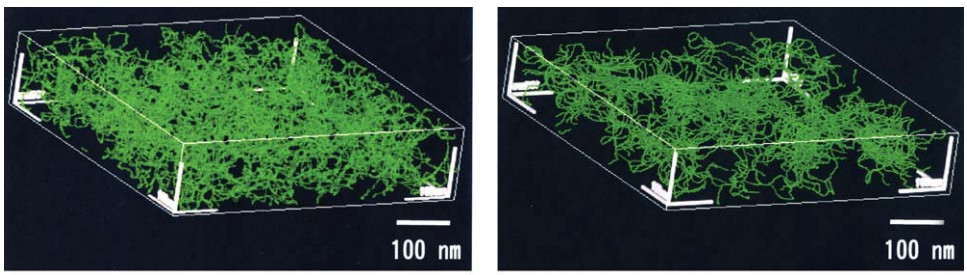

Figure 13 3D-TEM image analysis results for CB network of original CB-80 and heat-treated CB-80 at 383 K for 75 h in vacuum. (a) Original (b) Heat-treated. [Color figure can be viewed in the online issue, which is available at wileyonlinelibrary.com.]

than that of CB-50, and the more thermal stable composition is F_{cross} and F_{branch} = ca. 0.7 and ca. 0.3. Notice that CB-network structure is closely related to electric paths in rubber matrix. Therefore, these facts suggest that efficient electric paths of CB-50 are significantly severed in the process of the heat-treatment, whereas the damage of electric path of CB-80 is much lower than that of CB-50. This suggestion supports the dependence of the volume resistivities of CB-50 and CB-80 on the heat-treatment time at 383 K under vacuum.

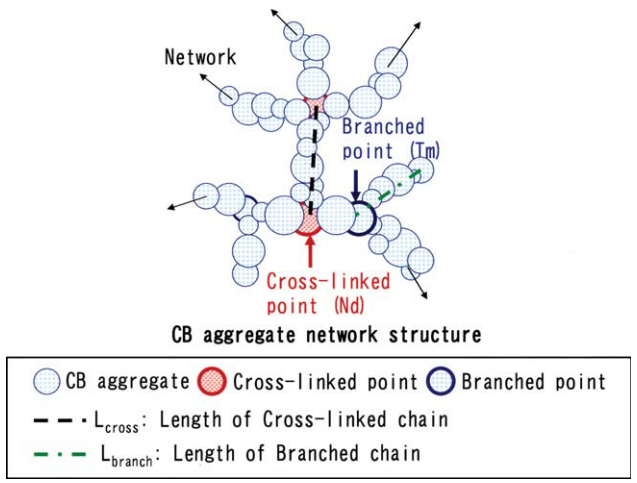

Figure 14 CB aggregate network and its parameters. [Color figure can be viewed in the online issue, which is available at wileyonlinelibrary.com.]

CONCLUSIONS

In this study, CB networks in rubbery matrix were visualized by 3D-TEM technique. It is shown that the heat-treatment under the temperature less than the thermal decomposition temperature of CB-filled NR vulcanizate has caused rearrangement of CB aggregates and/or thermal destruction of CB networks structure in rubber matrix by using the measurements of DSC, dynamic visco-elasticity and thermal expansion in the nitrogen atmosphere. Experimentally, the heat-treatment at 383 K under vacuum was chosen for further studying the thermal destruction of CB network in the rubbery matrix. Changes in the network structure induced by the heat-treatment were detected by the volume resistivity and 3D-TEM/electron tomography measurements.

Totally, 50 and 80 phr CB-filled natural rubber vulcanizates (CB-50 and CB-80) are much more electrically conductive than 0-10 phr CB-filled ones (CB-0, CB-5, and CB-10). Furthermore, the volume resistivity (ρ_v) of CB-50 increased rapidly up to a heat-treatment time of 24 h and it decreased by further heat-treatment, whereas the ρ_v of CB-80 remained almost constant without depending on heating time. Therefore, we used 3D-TEM observation technique as well as the volume resistivity measurement to investigate the CB structural change in CB-50 and CB-80 by the heat-treatment for 3 h or more at 383 K (110°C). It seemed that the CB network structure

TABLE III
Characteristics on CB Network of CB-50 and CB-80 Before/After Heat-Treatment at 383 K for 75 h in Vacuum by 3D-Image Analysis of 3D-TEM Images

Samples		L_{cross}/nm	L_{branch}/nm	D_{crss}[a]/nm^{-3}	D_{branch}[b]/nm^{-3}	F_{cross}[c]	F_{branch}[d]
CB-50	Original	40	82	8.0×10^{-6}	6.7×10^{-7}	0.94	0.06
	Heat-treated	23	42	2.0×10^{-5}	1.1×10^{-5}	0.68	0.32
CB-80	Original	39	110	1.7×10^{-5}	3.1×10^{-6}	0.88	0.12
	Heat-treated	22	46	3.0×10^{-5}	1.7×10^{-5}	0.67	0.33

[a,b] Densities of cross-linking points and branching points of CB network, respectively.
[c,d] Fractions of cross-linked chains and branched chains, respectively.

extended throughout the entire sample in the original CB-50 and CB-80, whereas the CB network in the heat-treated samples was markedly ruptured. Especially, thermal destruction of CB network structure is more remarkable in CB-50 than that in CB-80. It can be expected that this three-dimensional CB network structure formed by clustering of the CB aggregates is also closely related to various properties, in addition to electrical characteristics. Therefore, the crosslinked chains and the branched chains of the CB network were observed in CB-50 and CB-80 before/after the heat-treatment examined by 3D-TEM and 3D-image analysis.

Compared with the original nonheated samples, the average lengths (L_{cross} and L_{branch}) of the crosslinked chains and the branched ones, and the crosslinked points density (D_{cross}) of the heat-treated samples decreased, and the branched points density (D_{branch}) increased with decrease of D_{cross}. These reveal that the CB networks of CB-50 and CB-80 were broken and were rearranged by the heat-treatment. On the other hand, after the heat-treatment, the fractions (F_{cross}'s) of crosslinked chains of CB-50 and CB-80 decreased, whereas the fractions (F_{branch}'s) of the branched chains increased. These suggest that the heat-treatment changed the composition of their CB networks. Especially, F_{branch} of CB-50 became larger than that of CB-80, while the decrease of F_{cross} of CB-50 was almost the same as that of CB-80 by the heat-treatment. And, F_{cross} and F_{branch} of the heat-treated CB-50 were the same compositions (F_{cross} and F_{branch} = ca. 0.7 and ca. 0.3, respectively) as those of the heat-treated CB-80. It is suggested that the CB network of CB-80 is more thermal stable than that of CB-50, and the more thermal stable composition is F_{cross} and F_{branch} = ca. 0.7 and ca. 0.3. Considering that CB network structure is closely related to electric paths in rubber matrix, these facts suggest that efficient electric paths of CB-50 are significantly severed in the process of the heat-treatment, whereas the damage of electric path of CB-80 is much lower than that of CB-50. This suggestion supports the dependence of the volume resistivities of CB-50 and CB-80 on the heat-treatment time at 383 K under vacuum.

These results directly indicate that the CB networks were broken by the longer heat-treatment under vacuum. Destruction of the CB networks is closely related to the interaction between the CB filler and the rubbery matrix. The network was broken irreversibly if enough time was allowed to separate the CB aggregates beyond the distance of the interaction between them and the rubber. The techniques used in this study will become increasingly important for the rational design of the nano-composites of the rubbery matrix.

The authors thank Mr. H. Sawabe, Miss A. Isoda and Mr. M. Hashimoto (NISSAN ARC, LTD) and, Y. Kasahara and Y. Morita (KIT) for their valuable cooperations with this research.

References

1. Kraus, G. In Science and Technology of Rubber; Eirich, F. R., Ed. New York: Academic Press, 1978; p 339.
2. Kohjiya, S.; Senoo, K. In Compounding Design of Rubber and Nano-Composite. Kohjiya, S.; Nishi, T.; Yamaguchi, K.; Akiba, M., Eds.; CMC Publishing: Tokyo, 2007.
3. Kraus, G. Adv Polym Sci 1986, 8, 155.
4. Dannenberg, E. Chem Technol 1986, 59, 512.
5. Fukahori, Y. Nippon Gomu Kyokaishi 2004, 77, 19, 103, 180, 317.
6. Kaufman, S.; Slichter, W. P.; Davis, D. D. J Polym Sci Part B 1971, 9, 829.
7. Nishi, T. J Polym Sci Polym Part B 1974, 12, 685.
8. O'Brien, J.; Cashell, E.; Wardell, G. E.; McBriety, V. J Macromolecules 1976, 9, 653.
9. Serizawa, H.; Nakamura, T.; Ito, M.; Tanaka, K.; Nomura, A. Polym J 1983, 15, 543.
10. Sombatsompop, N.; Thongsang, S.; Markpin, T.; Wimolmala, E. J Appl Polym Sci 2004, 93, 2119.
11. Karásek, L.; Meissner, B.; Asai, S.; Sumita, M. Polymer J 1996, 28, 121.
12. Yamaguchi, K.; Busfield, J. J. C.; Thomas, A. G. J Polym Sci Phys Part B 2003, 41, 2079.
13. Satoh, Y.; Suda, K.; Fujii, S.; Kawahara, S.; Isono, Y.; Kagami, S. e-J Soft Mater 2007, 3, 29.
14. Treloar, L. R. G. The Physics of Rubber Elasticity, 2nd ed.; Clarendon: Oxford, 1958.
15. Tobolsky, A. V. Properties and Structure of Polymers. New York: Wiley, 1960.
16. Ferry, J. D. Viscoelastic Properties of Polymers, 3d ed. New York: Wiley, 1980.
17. Kohjiya, S.; Kato, A.; Ikeda, Y. Prog Polym Sci 2008, 33, 979.
18. Kohjiya, S.; Kato, A.; Suda, T.; Shimanuki, J.; Ikeda, Y. Polymer 2006, 47, 3298.
19. Kato, A.; Shimanuki, J.; Kohjiya, S. Rubber Chem Technol 2006, 79, 653.
20. Kohjiya, S.; Ikeda, Y.; Kato, A. In Current Topics in Elastomers Research, Chapter 19 Visualization of Nano-Filler Dispersion and Morphology in Rubbery Matrix by 3D-TEM; Bhowmick, A. K., Ed.; CRC Press: Boca Raton, London and New York, 2008; p 543.
21. Kato, A.; Ikeda, Y.; Kasahara, Y.; Shimanuki, J.; Suda, T.; Hasegawa, T.; Sawabe, H.; Kohjiya, S. J Opt Soc Am B 2008, 25, 1602.
22. Satoh, Y.; Suda, K., Fujii, S.; Kawahara, S.; Isono, Y.; Kagami, S. e-J Soft Mater 2007, 3, 14.
23. Gent, A. N. Engineering with Rubber; Hanser Publishers; Munich, 1992.
24. Kreakley, P. K.; Payne, A. R. Theory and Practice of Engineering with Rubber; Applied Science Pub.: London, 1978.
25. Isono, Y.; Ferry, J. D. Rubber Chem Technol 1984, 57, 925.
26. Ghani, A. A.; Eatha, A. I.; Hassan, A. A. Angew Makromol Chem 1985, 129, 1.
27. Waddell, W. H.; Evans, L. R. Rubber Chem Technol 1996, 69, 377.
28. Medalia, A. I. In Mixing and Compounding of Polymers—Theory and Practice; Manas-Zloczower, I.; Tadmor, Z., eds.; Hanser Publishers: Munich, 1994.
29. Bergna, H. E., ed. In Adv in Chemistry Series 234; American Chem Society: Washington, DC, 1994.

30. Payne, A. R. J Appl Polym Sci 1965, 9, 2273.
31. Piau, J. M.; Dorget, M.; Paliene, J. F.; Pouchelon, A. J Rheol 1999, 43, 305.
32. Aranguren, M. I.; Mora, E. M.; DeGroot, J. V.; Macosko, C. W. J Rheol 1992, 36, 1165.
33. Cassagnau, P.; Mélis, F. Polymer 2003, 44, 6607.
34. Gurovich, D.; Macosko, C. W.; Tirrell, M. Rubber Chem Technol 2003, 76, 1.
35. Sarvestani, A. S.; Picu, C. R. Polymer 2004, 45, 7779.
36. Yan, H. X.; Sun, K.; Zhang, Y. Polym Test 2005, 24, 32.
37. Chabert, E.; Dendievel, R.; Gauthier, C.; Cavail&edot, J. Y. Compos Sci Technol 2004, 64, 316.
38. Scurati, A.; Zloczower, I. M. Rubber Chem Technol 2001, 75, 725.
39. Poh, B. T.; Keok, C. P.; Lim, G. H. Eur Polym Mater 1995, 31, 223.
40. Poh, B. T.; Ismail, H.; Tan, K. S., Polym Test 2002, 21, 801.
41. da Silva, A. L. N.; Rocha, M. M. C. G.; Moraes, M. A. R. C.; Valente, C. A. R.; Coutinho, F. M. B. Polym Test 2002, 21, 57.
42. Thomas, P. S.; Streekumar, P. A.; Thomas, S.; Aprem, A. S.; Yang, W. Molecular transport characteristics of poly(ethylene co-vinyl acetate)/ calcium phosphate nanocomposites in different solvents, The Accademic Review of ST. Berchmans Cllege: Available at: //www.sbcollege.org/accademicreview.html.
43. Dionne, P. J.; Picu, C. R.; Ozisik, R. Macromolecules 2006, 39, 3089.
44. Marier, P. G.; Göritz, D. Kautsch Gummi Kunstst 1996, 49, 18.
45. Havet, G.; Isayev, A. I. Rheol Acta 2001, 40, 570.
46. Fujiwara, S.; Fujimoto, K. Rubber Chem Technol 1971, 44, 1273.
47. Kaufman, S.; Slichter, W. P.; Davis, D. O. J Polym Sci A2 1971, 8, 829.
48. Simhambhatla, M.; Leonov, A. I. Rheol Acta 1995, 34, 329.
49. Zhang, Q.; Archer, L. Langmuir 2002, 18, 10435.
50. Zhang, Q.; Archer, L. Macromolecules 2004, 37, 1928.
51. Steinstein, S. S.; Zhu, A. Macromolecules 2002, 35, 7262.
52. Zhu, Z.; Thompson, T.; Wang, S. Q.; von Meerwall, E. D.; Halasa, A. Macromolecules 2005, 38, 8816.
53. Fukahori, Y. In Current Topics in Elastomers Research, 18 Mechanism of the Carbon Black Reinforcement of Rubbers; Bhowmick, A. K., Ed., CRC Press: Boca Raton, London and New York, 2008; p 518–539.
54. Klüppel, M. Adv Polym Sci 2003, 164, 1.
55. Klüppel, M.; Heinrich, G. Kautsch Gummi Kunstst 2005, 58, 217.
56. Feinrich, G.; Klüppel, M. Adv Polym Sci 2002, 160, 1.
57. Montes, H.; Lequeux, F.; Berriot, J Macromolecules 2003, 36, 8107.
58. Lee, B. L. In Mixing and Compounding of Polymers—Theory and Practice; Manas-Zloczower, I.; Tadmor, Z., Eds.; Hanser Publishers: Munich, 1994.
59. http//www.sakai-chem.co.jp/product/muki_aen.html.
60. Watanabe, S. Nippon Gomu Kyoukaishi 1961, 34, 787.
61. Flory, P. J.; Rehner, J. J. J Chem Phys 1943, 11, 521.
62. Coran, A. Y. J Appl Polym Sci 2003, 87, 24.
63. Coran, A. Y. In Vulcanization Science and Technology of Rubber, 2nd ed. Mark, J. E.; Erman, B.; Eirich, F. R., Eds.; Academic Press: San Diego, 1994.
64. Ikeda, Y.; Kato, A.; Shimanuki, J.; Kohjiya, S. Macromol Rapid Commun 2004, 25, 1186.
65. Kohjiya, S.; Kato, A.; Shimanuki, J.; Hasegawa, T.; Ikeda, Y. Polymer 2005, 46, 4440.
66. Kohjiya, S.; Kato, A.; Shimanuki, J.; Hasegawa, H.; Ikeda, Y. J Mater Sci 2005, 40, 2553.
67. Kato, A.; Ikeda, Y.; Kohjiya, S. Nippon Gomu Kyokaishi 2005, 78, 180.
68. Tsuji, M.; Kohjiya, S. Prog Polym Sci 1995, 20, 259.
69. Tsuji, M.; Fujita, M.; Kohjiya, S. Nihon Reoroji Gakkaishi 1997, 25, 193.
70. The Boulder Laboratory for 3-Dimensional Electron Microscopy of Cells and Regents of the University of Colorado, The IMOD Home Page, Available at: http://bio3d.colorado.edu/imod/.
71. The Mercury Visualization Sciences, Visualization Software, Available at: http://www.tgs.com/.
72. Farmer, E. H.; Shipley, F. W. J Polym Sci 1946, 1, 293.
73. Payne, A. R.; Whittaker, R. E. Rubber Chem Technol 1971, 44, 440.
74. McDonald, G.; Hess, W. Rubber Chem Technol 1977, 50, 842.
75. Kraus, G. Rubber Chem Technol 1978, 51, 297.
76. Rivin, D.; Aron, J.; Medalia, A. I. Rubber Chem Technol 1968, 41, 330.
77. Ban, L. L.; Hess, W. M.; Papazian, L. A. Rubber Chem Technol 1974, 47, 858.
78. Printer, P. E.; McGill, G. R. Rubber World 1978, 30, 177.
79. Pérez, L. D.; Sierra, L.; Lopez, B. L. Published online in Wiley InterScience 2008, wileyonlinelibrary.com.
80. Ghosh, P.; Chakrabarti, A. Eur Polym J 2000, 36, 1043.
81. Kimura, T.; Sone, M.; Mitsui, H.; Ichikawa, K. Relationship between mechanical properties and electric properties of natural rubber. Document of Electric Discharge Meeting of the Institute of Electric Engineers of Japan 1983; ED-83.
82. Mohanraj, G. T.; Chaki, T. K.; Chakraborty, A.; Khastgir, D. J Appl Polym Sci 2004, 92, 2179.